

Discriminator-free Unsupervised Domain Adaptation for Multi-label Image Classification

Inder Pal Singh¹, Enjie Ghorbel¹, Anis Kacem¹, Arunkumar Rathinam¹ and Djamila Aouada¹

¹University of Luxembourg

{inder.singh, enjie.ghorbel, anis.kacem, arunkumar.rathinam, djamila.aouada}@uni.lu

Abstract

In this paper, a discriminator-free adversarial-based Unsupervised Domain Adaptation (UDA) for Multi-Label Image Classification (MLIC) referred to as DDA-MLIC is proposed. Over the last two years, some attempts have been made for introducing adversarial-based UDA methods in the context of MLIC. However, these methods which rely on an additional discriminator subnet present two shortcomings. First, the learning of domain-invariant features may harm their task-specific discriminative power, since the classification and discrimination tasks are decoupled. Moreover, the use of an additional discriminator usually induces an increase of the network size. Herein, we propose to overcome these issues by introducing a novel adversarial critic that is directly deduced from the task-specific classifier. Specifically, a two-component Gaussian Mixture Model (GMM) is fitted on the source and target predictions in order to distinguish between two clusters. This allows extracting a Gaussian distribution for each component. The resulting Gaussian distributions are then used for formulating an adversarial loss based on a Fréchet distance. The proposed method is evaluated on five multi-label image datasets. The obtained results demonstrate that DDA-MLIC outperforms existing state-of-the-art methods in terms of precision while requiring a lower number of parameters. The code will be made publicly available online¹.

1 Introduction

Multi-Label Image Classification (MLIC) aims at predicting the presence/absence of a set of objects in a given image. It is widely studied in the Computer Vision community due to its numerous fields of applications such as object recognition [Bell *et al.*, 2016], scene classification [Shao *et al.*, 2015] and attribute recognition [Li *et al.*, 2016].

With the latest advancements in deep learning, several MLIC methods [He *et al.*, 2016; Ridnik *et al.*, 2021b;

Ridnik *et al.*, 2021a] have achieved remarkable performance on well-known datasets [Lin *et al.*, 2014; Everingham *et al.*, 2010]. Nevertheless, the effectiveness of deep learning-based methods widely relies on the availability of annotated datasets. This requires costly and time-consuming efforts. As a result, given the limited number of labelled data, existing MLIC methods tend to have poor generalization capabilities to unseen domains. This problem is commonly known as *domain-shift*, where a method trained on a *source* dataset fails to generalize on a *target* one belonging to a different domain. To overcome this issue, *Unsupervised Domain Adaptation (UDA)* [Ganin *et al.*, 2016; Pei *et al.*, 2018] can be an interesting strategy. The idea behind UDA consists in leveraging unlabeled data from the target dataset in order to reduce the gap between the source and the target domains.

In the literature, many works have been proposed for UDA in the context of single-label image classification [Ganin *et al.*, 2016; Pei *et al.*, 2018; Saito *et al.*, 2018; Long *et al.*, 2018; Long *et al.*, 2015], while less efforts have been dedicated to proposing UDA methods that are suitable for MLIC. Inspired by the predominance of adversarial-based approaches in single-label image classification, few methods [Lin *et al.*, 2021; Pham *et al.*, 2021] have attempted to extend UDA to MLIC. Similar to [Ganin *et al.*, 2016], these adversarial approaches leverage a domain discriminator for implicitly reducing the domain gap. In particular, a min-max two-player game guides the generator to extract domain-invariant features that fool the discriminator. Nevertheless, this may come at the cost of decreasing their task-specific discriminative power, as highlighted in [Chen *et al.*, 2022]. In addition, using an additional discriminator will naturally lead to an increase in the network size. Chen *et al.* [Chen *et al.*, 2022] attempted to solve this problem in the context of single-label image classification by implicitly reusing the classifier as a discriminator. In particular, they considered the difference between inter-class and intra-class correlations of the classifier probability predictions as an adversarial critic. While this approach is promising, generalizing it to MLIC is not straightforward, as the per-class prediction probabilities are not linearly dependent (they do not sum up to one) making their correlation hardly interpretable.

In this paper, we introduce a discriminator-free adversarial UDA approach for MLIC based on a novel adversarial critic.

¹anonymous.4open.science/r/DDA-MLIC-Anonymous

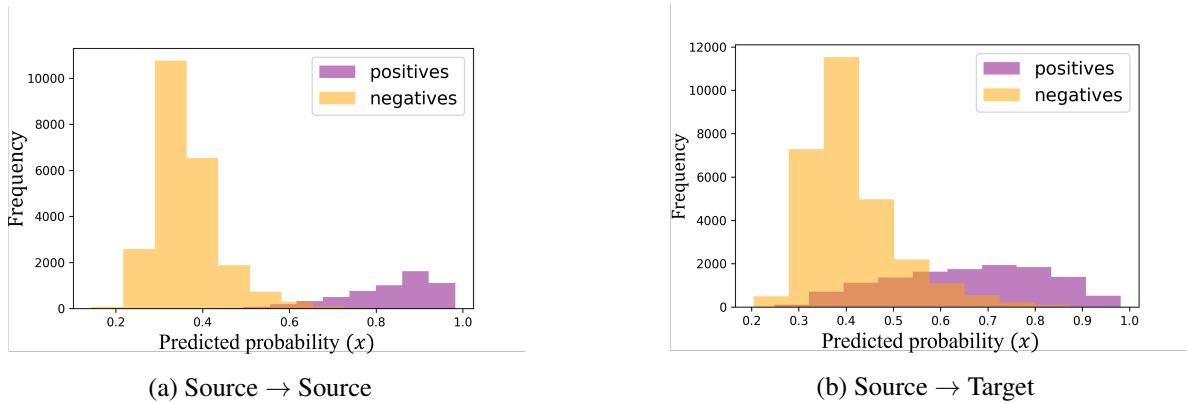


Figure 1: Histogram of classifier predictions. Predicted probabilities using source-only trained classifier² on: a) source dataset³ (\mathcal{I}_s), and b) target dataset³ (\mathcal{I}_t).

As in [Chen *et al.*, 2022], we propose to leverage the task-specific classifier for defining the adversarial critic. However, instead of relying on the prediction correlations which do not apply to the case of MLIC, we propose to fit a Gaussian Mixture Model (GMM) with two components on both the source and target predictions. A Fréchet distance [Dowson and Landau, 1982] between the estimated pair of components is then used to define the proposed discrepancy measure. This intuition comes from the fact that source data are usually more confidently classified (as positive or negative) than target ones, as illustrated in Fig. 1. The same figure also highlights that the distribution of predictions can be modeled by two clusters; hence, demonstrating the interest of using a two-component GMM. The experimental results show that we outperform state-of-the-art methods in terms of precision, while significantly reducing the number of network parameters.

In summary, our contributions are:

- a novel domain discrepancy for multi-label image classification based on the distribution of the task-specific classifier predictions;
- an effective and efficient adversarial unsupervised domain adaptation method for multi-label image classification. The proposed adversarial strategy does not require an additional discriminator, hence reduces the network size;
- an experimental quantitative and qualitative analysis on several benchmarks showing that the proposed method outperforms state-of-the-art works.

The rest of the paper is organized as follows. Section 3 formulates the problem of domain adaptation for multi-label image classification, and presents our intuition behind using the classifier as a critic. Section 4 introduces the proposed approach termed DDA-MLIC. The experimental results are reported and discussed in Section 5. Finally, Section 6 concludes this work and draws some perspectives.

²Classifier: TResNet-M [Ridnik *et al.*, 2021b] trained on UCM [Chaudhuri *et al.*, 2017] dataset.

³Source: UCM [Chaudhuri *et al.*, 2017] validation set (420 im-

2 Related works

In this section, we review the state-of-the-art of the general topic of unsupervised domain adaptation. Then, we discuss existing unsupervised domain adaptation methods that were specifically designed for the case of multi-label image classification.

2.1 Unsupervised domain adaptation

Recent unsupervised domain adaptation techniques can be categorized into four main classes: moment-matching [Tzeng *et al.*, 2014; Long *et al.*, 2015; Zhang *et al.*, 2019], self-training [Sun *et al.*, 2019; Kang *et al.*, 2019], image-to-image translation [Murez *et al.*, 2018; Li *et al.*, 2019], and adversarial methods [Ganin *et al.*, 2016; Du *et al.*, 2021; Tang and Jia, 2020; Lee *et al.*, 2019; Chen *et al.*, 2022]. The first category aims at learning domain-invariant features by explicitly aligning the feature distributions of the source and the target domains. This is usually done by defining a moment-based distribution discrepancy between the two domains such as Maximum Mean Discrepancy (MMD) [Tzeng *et al.*, 2014], Multi-Kernel Maximum Mean Discrepancy (MK-MMD) [Long *et al.*, 2015] and Joint Maximum Mean Discrepancy (JMMD) [Zhang *et al.*, 2019]. On the other hand, self-training techniques employ self-supervision for reducing the domain discrepancy. This can be done by defining a relevant pretext task [Sun *et al.*, 2019]; hence generating pseudo-labels that are used to train the feature extractor. Alternatively, contrastive learning techniques are also investigated [Kang *et al.*, 2019]. Image-to-image translation approaches leverage Generative Adversarial Networks (GAN) to generate synthetic target images from the source data [Murez *et al.*, 2018; Li *et al.*, 2019]. Taking another direction, adversarial methods make use of an additional classifier usually referred to as discriminator which is trained for distinguishing between source and target images [Ganin *et al.*, 2016]. A min-max game between this discriminator and the task-specific classifier/regressor is then carried out in order to implicitly learn domain-invariant features. Given

their good performance, especially in the context of classification, impressive efforts have been made for developing more advanced adversarial-based variants [Du *et al.*, 2021; Tang and Jia, 2020; Lee *et al.*, 2019].

In [Chen *et al.*, 2022], it is suggested that decoupling the discriminator and the task-specific classifier may cause mode collapse. As a solution, Chen *et al.* [Chen *et al.*, 2022] have introduced a new paradigm, namely, a discriminator-free adversarial unsupervised domain adaptation. They have proposed to reuse the classifier as a discriminator by defining a critic based on the classifier predictions. In particular, they showed that the difference between the intra-class and inter-class correlations can be considered as a domain discrepancy. In the context of single-label classification, the proposed discriminator-free adversarial strategy achieved impressive results while reducing the network size. Nevertheless, generalizing it to the task of multi-label classification is tricky. Indeed, the self-correlation matrix used to define intra-class and inter-class correlations is computed based on prediction probabilities. For each sample, the sum of these prediction probabilities should be equal to one. While this assumption can be imposed in the context of single-label classification, it does not hold for multi-label image classification, as several labels can appear at the same time in a given image.

2.2 Unsupervised domain adaptation for multi-label image classification

Despite the popularity of unsupervised domain adaptation, less efforts have been made for investigating this topic in the context of multi-label image classification [Pham *et al.*, 2021; Lin *et al.*, 2021; Singh *et al.*, 2023]. Taking inspiration from single-label image classification, existing approaches [Pham *et al.*, 2021; Lin *et al.*, 2021; Singh *et al.*, 2023] mostly extend the classical multi-label classification framework by adopting an adversarial learning strategy. Specifically, an additional discriminator is considered for differentiating the source and target domains. As in [Ganin *et al.*, 2016; Tang and Jia, 2020], a min-max game is often adopted for training the discriminator. Nevertheless, as discussed in [Chen *et al.*, 2022], considering the discriminator and the task-specific classifier as two standalone subnetworks [Pham *et al.*, 2021; Lin *et al.*, 2021; Singh *et al.*, 2023] may also result in mode collapse while enlarging the overall network size.

3 Problem formulation and motivation

3.1 Problem formulation

Let $\mathcal{D}_s = (\mathcal{I}_s, \mathcal{Y}_s)$ and $\mathcal{D}_t = (\mathcal{I}_t, \mathcal{Y}_t)$ be the source and target datasets, respectively, with P_s and P_t being their respective probability distributions such that $P_s \neq P_t$. Let us assume that they are both composed of N object labels. Note that $\mathcal{I}_s = \{\mathbf{I}_s^k\}_{k=1}^{n_s}$ and $\mathcal{I}_t = \{\mathbf{I}_t^k\}_{k=1}^{n_t}$ refer to the sets of n_s source and n_t target image samples, respectively, while $\mathcal{Y}_s = \{\mathbf{y}_s^k\}_{k=1}^{n_s}$ and $\mathcal{Y}_t = \{\mathbf{y}_t^k\}_{k=1}^{n_t}$ are their associated sets of labels.

Let us denote by \mathcal{I} the set of all images such that $\mathcal{I} = \mathcal{I}_s \cup \mathcal{I}_t$. Given an input image $\mathbf{I} \in \mathcal{I}$ with $\mathbf{y} \in \{0, 1\}^N$ being its label, the goal of *unsupervised domain adaptation*

for *multi-label image classification* is to estimate a function $f : \mathcal{I} \mapsto \{0, 1\}^N$ such that,

$$f(\mathbf{I}) = \mathbb{1}_{f_c \circ f_g(\mathbf{I}) > \tau} = \mathbb{1}_{\mathbf{X} > \tau} = \mathbf{y}, \quad (1)$$

where $f_g : \mathcal{I} \mapsto \mathbb{R}^d$ extracts d -dimensional features, $f_c : \mathbb{R}^d \mapsto [0, 1]^N$ predicts the probability of object presence, $\mathbf{X} = f_c \circ f_g(\mathbf{I}) \in [0, 1]^N$ corresponds to the logits, $\mathbb{1}$ is an indicator function, $>$ is a comparative element-wise operator with respect to a chosen threshold τ . Note that only \mathcal{D}_s and \mathcal{I}_t are used for training. In other words, the target dataset is assumed to be unlabeled.

To achieve this goal, some existing methods [Lin *et al.*, 2021; Singh *et al.*, 2023] have adopted an adversarial strategy by considering an additional discriminator f_d that differentiates between source and target data. Hence, the model is optimized using a classifier loss \mathcal{L}_c such as the asymmetric loss (ASL) [Ridnik *et al.*, 2021a] and an adversarial loss \mathcal{L}_{adv} defined as,

$$\mathcal{L}_{adv} = \mathbb{E}_{f_g(\mathbf{I}_s) \sim \bar{P}_s} \log \frac{1}{f_d(f_g(\mathbf{I}_s))} + \mathbb{E}_{f_g(\mathbf{I}_t) \sim \bar{P}_t} \log \frac{1}{(1 - f_d(f_g(\mathbf{I}_t)))}, \quad (2)$$

where \bar{P}_s and \bar{P}_t are the distributions of the learned features from source and target samples \mathcal{I}_s and \mathcal{I}_t , respectively.

While the adversarial paradigm has shown great potential [Lin *et al.*, 2021], the use of an additional discriminator f_d which is decoupled from f_c may lead to mode collapse as discussed in [Chen *et al.*, 2022]. Inspired by the work of [Chen *et al.*, 2022], we aim at addressing the following question – *Could we leverage the outputs of the task-specific classifier $f_c \circ f_g$ in the context of multi-label classification for implicitly discriminating the source and the target domains?*

3.2 Motivation: domain discrimination using the distribution of the classifier logits

The goal of MLIC is to identify the classes that are present in an image (*i.e.*, *positive labels*) and reject the ones that are not present (*i.e.*, *negative labels*). Hence, the classifier f_c is expected to output high probability values (logits) for the positive labels and low probability values for the negative ones. Formally, let $x = \sigma(f_c(f_g(\mathbf{I}))) = \sigma(\mathbf{X}) \sim \hat{P}$ be the random variable modelling the predicted probability (logits) of any class and \hat{P} its probability distribution, with σ being a uniform random sampling function that returns the predicted probability of a randomly selected class. In general, a well-performing classifier is expected to classify confidently both negative and positive samples. Ideally, this would mean that the probability distribution \hat{P} should be formed by two clusters with low variance in the neighborhood of 0 and 1, respectively denoted by \mathcal{C}_0 and \mathcal{C}_1 . Hence, our hypothesis is that a drop in the classifier performance due to a domain shift can be reflected in \hat{P} .

Let $x_s = \sigma(f_c(f_g(\mathbf{I}_s))) \sim \hat{P}_s$ and $x_t = \sigma(f_c(f_g(\mathbf{I}_t))) \sim \hat{P}_t$ be the random variables modelling the logits obtained from the source and target data and \hat{P}_s and \hat{P}_t be their distributions, respectively. Concretely, we propose to investigate

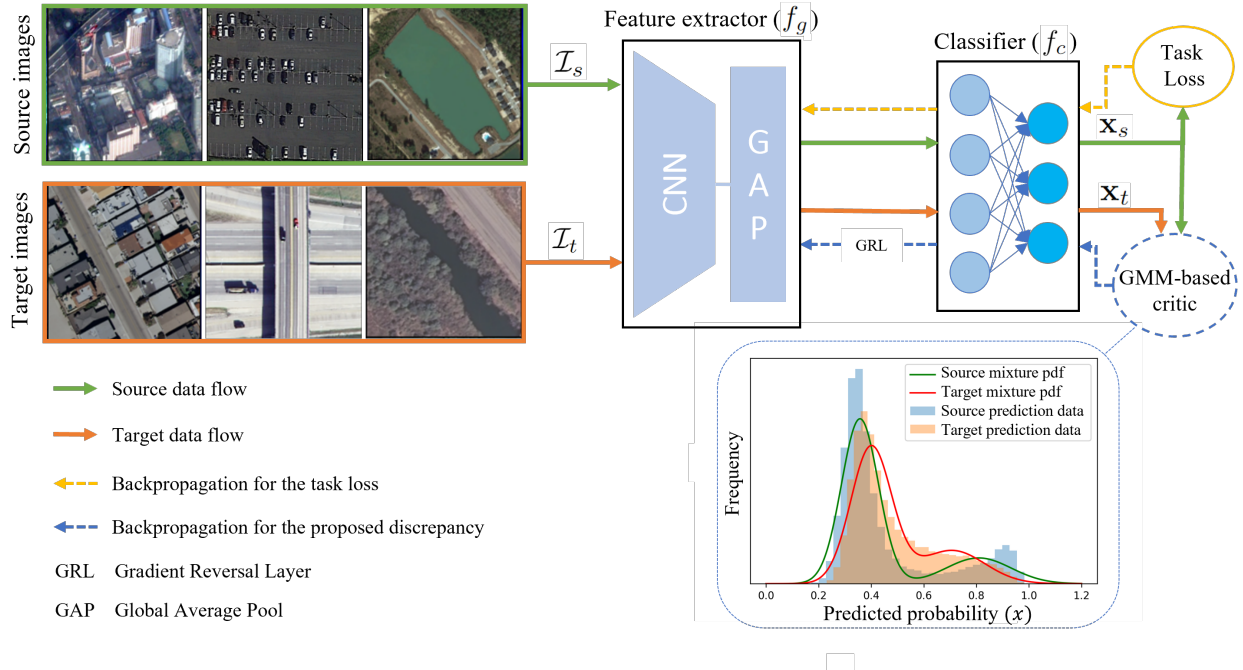


Figure 2: Overall proposed architecture: The feature extractor (f_g) learns discriminative features from source and target images. The task classifier (f_c) performs two actions simultaneously: 1) it learns to classify source samples correctly using a supervised task loss, and 2) when used as a discriminator, it aims to minimize/maximize the proposed discrepancy between source and target predictions.

whether the shift between the source and target domains is translated in \hat{P}_s and \hat{P}_t . If a clear difference is observed between \hat{P}_s and \hat{P}_t , this would mean that the classifier f_c should be able to discriminate between source and target samples. Thus, this would allow the definition of a suitable critic directly from the classifier predictions.

To support our claim, we trained⁴ a model f using the labelled source data \mathcal{D}_s without involving the target images \mathcal{I}_t ⁵. In Fig. 1 (a), we visualize the histogram of the classifier probability outputs x_s and x_t when the model is tested on the source domain. It can be clearly observed that the logits on the source domain, denoted by x_s , can be grouped into two separate clusters. Fig. 1 (b) shows the same histogram when the model is tested on target samples. In contrast to the source domain, the classifier probability outputs, denoted by x_t , are more spread out in the target domain. In particular, the two clusters are less separable than in the source domain. This is due to the fact that the classifier f_c benefited from the supervised training on the source domain, and as a result it gained an implicit discriminative ability between the source and target domains.

Motivated by the observations discussed above, we propose to reuse the classifier to define a critic function based on \hat{P}_s and \hat{P}_t . In what follows, we describe our approach including the probability distribution modelling (\hat{P}_s and \hat{P}_t) and the adversarial strategy for domain adaptation.

⁴Classifier: TRResNet-M [Ridnik *et al.*, 2021b] trained on UCM [Chaudhuri *et al.*, 2017] dataset.

⁵Source: UCM [Chaudhuri *et al.*, 2017] validation set (420 images), Target: AID [Hua *et al.*, 2020] validation set (600 images).

4 An Implicit Multi-Label domain adaptation adversarial strategy

As discussed in Section 3.2, the classifier probability predictions are usually formed by two clusters. Consequently, as shown in Fig. 3 (a), we propose to approximate the distributions \hat{P}_s and \hat{P}_t by a two-component Gaussian Mixture Model (GMM) [Reynolds, 2009] as follows,

$$\hat{P}_s(x_s) \approx \sum_{i=1}^2 w_i^s \mathcal{N}(x_s | \mu_i^s, \Sigma_i^s), \quad (3)$$

and,

$$\hat{P}_t(x_t) \approx \sum_{i=1}^2 w_i^t \mathcal{N}(x_t | \mu_i^t, \Sigma_i^t), \quad (4)$$

where $\mathcal{N}(x_t | \mu_i^t, \Sigma_i^t)$ denotes the i -th Gaussian distribution, with the mean μ_i^t and the variance Σ_i^t , fitted on the target logits x_t and w_i^t its mixture weight such that $w_1^t + w_2^t = 1$. Similarly, $\mathcal{N}(x_s | \mu_i^s, \Sigma_i^s)$ denotes the i -th Gaussian distribution, with the mean μ_i^s and the variance Σ_i^s , fitted on the source logits x_s and w_i^s its mixture weight such that $w_1^s + w_2^s = 1$. An Expectation-Maximization (EM) algorithm [Reynolds, 2009] is used to estimate the GMM parameters. In both source and target domains, we assume that the first component of the GMM corresponds to the cluster \mathcal{C}_0 (with a mean close to 0), while the second corresponds to \mathcal{C}_1 (with a mean close to 1).

However, due to a large number of negative predictions as compared to positive ones, the component \mathcal{C}_0 tends to be more dominant. In fact, in a given image, only few objects are usually present from the total number of classes. To alleviate

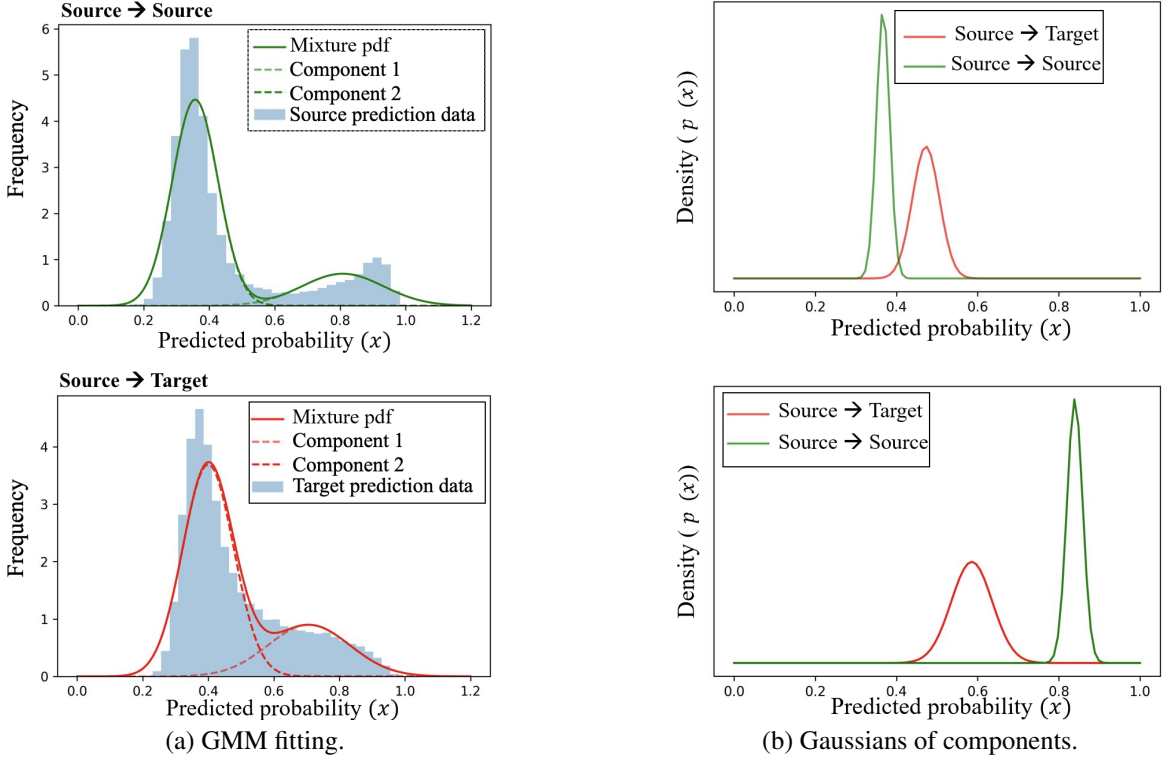


Figure 3: a) The classifier¹ predictions x_s and x_t for both source and target datasets², respectively, can be grouped into two clusters. Hence, a two-component GMM can be fitted for both source (\hat{P}_s) and target (\hat{P}_t). While the first component is close to 0, the second is close to 1, b) A component-wise comparison between source (\hat{P}_s^1, \hat{P}_s^2) and target (\hat{P}_t^1, \hat{P}_t^2) Gaussians of distributions extracted from the fitted GMM confirms that target predictions are likely to be farther from 0 and 1 with a higher standard deviation than the source.

this phenomenon, we propose to extract two Gaussian components from the source and target GMM, ignoring the estimated weights illustrated in Fig. 3 (b). Hence, we propose to redefine the adversarial loss \mathcal{L}_{adv} by computing a Fréchet distance d_F [Dowson and Landau, 1982] between each pair of source and target components from a given cluster as follows.

$$\mathcal{L}_{adv} = \sum_{i=1}^2 \alpha_i d_F(\mathcal{N}(x_t | \mu_i^t, \Sigma_i^t), \mathcal{N}(x_s | \mu_i^s, \Sigma_i^s)), \quad (5)$$

with α_i weights that are empirically fixed. The Fréchet distance, also referred to as 2-Wasserstein distance, is chosen as it allows computing the distance between two probability distributions. In addition, as compared to the commonly used 1-Wasserstein distance [Arjovsky *et al.*, 2017], it takes into account second-order moments. Since the computed distributions are univariate Gaussians, the Fréchet distance between two distributions is defined as follows,

$$d_F^2(\mathcal{N}(x_1 | \mu_1, \Sigma_1), \mathcal{N}(x_2 | \mu_2, \Sigma_2)) = (\mu_1 - \mu_2)^2 + (\sigma_1 - \sigma_2)^2, \quad (6)$$

where $\mathcal{N}(x_1 | \mu_1, \Sigma_1)$ and $\mathcal{N}(x_2 | \mu_2, \Sigma_2)$ are two Gaussians with a mean of μ_1 and μ_2 and a standard deviation of Σ_1 and Σ_2 , respectively.

The overall architecture of the proposed method is shown in Fig. 2. Similar to [Chen *et al.*, 2022], our network con-

sists of a feature extractor f_g that aims to extract discriminative image features from source \mathcal{D}_s and target \mathcal{I}_t datasets and a classifier f_c that simultaneously performs the classification and discriminates between source and target features by minimizing the proposed adversarial loss \mathcal{L}_{adv} . A Gradient Reversal Layer (GRL) between f_g and f_c enforces the feature extractor to fool the classifier, when acting as a discriminator, hence implicitly learning domain-invariant features.

5 Experiments

5.1 Implementation details

A lightweight version of TRResNet [Ridnik *et al.*, 2021b], called TRResNet-M, has been used as the feature extractor. Given its impressive performance in multi-label image classification, the Asymmetric Loss (ASL) [Ridnik *et al.*, 2021a] has been used as the loss function for the classification task. The model is trained using the Adam optimizer with a cosine decayed maximum learning rate of 10^{-3} for a total of 40 epochs or until convergence.

5.2 Datasets

Two types of datasets have been used in our experiments, namely 3 aerial image datasets as well as 2 urban street datasets.

Aerial image datasets

AID Dataset: A multi-label version of the original AID dataset [Xia *et al.*, 2017] was proposed in [Hua *et al.*, 2020], where 3000 aerial images have been selected and annotated with multiple objects from a list of 17 categories. The size of the images is equal to 600×600 pixels with a spatial resolution of 0.5 m/pixel to 8 m/pixel. The 17 categories are: airplane, sand, pavement, buildings, cars, chaparral, court, trees, dock, tank, water, grass, mobile-home, ship, bare-soil, sea, and field.

UCM Dataset: Originally introduced for the purpose of multi-class classification with a total of 2100 image samples [Yang and Newsam, 2010], a multi-label version of the UCM dataset was proposed in [Chaudhuri *et al.*, 2017]. The manually assigned labels were taken from a total of 17 categories, similar to the AID dataset. Having an image size of 300×300 pixels and a pixel resolution of one foot, UCM is a good candidate for domain adaptation as it slightly differs from the AID dataset.

DFC15 Dataset: This multi-label aerial image dataset comes with 3342 high resolution images labelled from a total of 8 categories [Hua *et al.*, 2019]. Similar to the two previous datasets, UCM was originally introduced for multi-class classification in 2015. The images were acquired using Zeebrugge with an airborne sensor, which is 300m off the ground having a size of 10000×1000 with a spatial resolution of 5 cm. The given 8 category labels are: impervious, water, clutter, vegetation, building, tree, boat, and car. In our experiments, we make use of the 6 common categories between DFC15 and the two other datasets.

Urban street dataset

Unlike single-label image classification, datasets for evaluating domain adaptation methods for multi-label image classification are sparse. Hence, we consider two widely used urban street datasets, namely CityScapes [Cordts *et al.*, 2016] and GTA5 [Richter *et al.*, 2016]. These datasets were originally introduced for the purpose of semantic image segmentation. In order to employ them in the context of multi-label image classification, the segmented objects are converted to classes.

CityScapes Dataset: This dataset [Cordts *et al.*, 2016] is composed of 5000 real images that have been captured in daytime and have been annotated at the pixel-level. It includes 19 categories. The objects that are present in all the image samples are not considered in our experiments. Hence, we reduce the number of category labels to 11 and generate label classes. This dataset is used as target dataset in our experiments.

GTA5 Dataset: GTA5 dataset [Richter *et al.*, 2016] provides 24966 synthetic images rendered using the open-world video game Grand Theft Auto 5. Similar to the CityScapes, we generate a multi-label version of the GTA5 dataset considering the same 11 categories. This dataset is used as source dataset in our experiments.

5.3 Comparison with the state-of-the-art

We compare the proposed approach with existing state-of-the-art methods in terms of number of model parameters, mean Average Precision (mAP), average per-Class Precision

(CP), average per-Class Recall (CR), average per-Class F1-score (CF1), average Overall Precision (OP), average overall recall (OR) and average Overall F1-score (OF1). Classical Multi-Label Image Classification (MLIC) methods are considered, as well as Domain Adaptation-based approaches (DA). Given the five considered datasets, *i.e.*, AID, UCM, DFC15, GTA5 and Cityscapes, five experimental settings are considered, *i.e.*, AID \rightarrow UCM, UCM \rightarrow AID, AID \rightarrow DFC15, UCM \rightarrow DFC15, and GTA5 \rightarrow CityScapes. For instance, AID \rightarrow UCM indicates that during the training AID is fixed as the source dataset while UCM is considered as the target one. The results are reported on the testing set of the target dataset.

Table 1, Table 2, and Table 3 quantitatively compare the proposed approach to state-of-the-art methods. It can be clearly seen that our model requires fewer parameters, with a total of 31.4 million trainable parameters. Moreover, our method termed DDA-MLIC achieves the best performance in terms of mAP for AID \rightarrow UCM, UCM \rightarrow AID, UCM \rightarrow DFC and GTA5 \rightarrow CityScapes. Moreover, the per-class average scores, *i.e.*, CP, CR and CF1, are the highest among all for AID \rightarrow UCM and UCM \rightarrow DFC. Additionally, the per-example or overall average scores, *i.e.*, OP, OC and OF1, are the highest for the latter among current methods. However, for the AID \rightarrow DFC setting, DDA-MLIC ranks second in terms of mAP after DA-MAIC [Lin *et al.*, 2021]. This might be explained by the presence of an important class imbalance in the AID dataset. Since DDA-MLIC relies on the alignment of the distribution of source and target predictions, the proposed method can be highly impacted by the class imbalance. This problem will be further analyzed in future works.

5.4 Qualitative analysis

In order to qualitatively analyze the effectiveness of the proposed approach, we visualize in Fig. 4 the source and target prediction distributions before and after applying domain adaptation. It can be clearly seen that the distribution of target predictions (red in color) is shifting towards source distribution (solid red to dotted red) for both positive and negative samples.

5.5 Ablation study

The results of the ablation study are shown in Table 4. We report the obtained mAP for all the four considered settings, *i.e.*, AID \rightarrow UCM, UCM \rightarrow AID, UCM \rightarrow AID and UCM \rightarrow DFC. The first row shows the mAP obtained in the absence of any domain adaptation strategy. The second row includes the scores obtained when adopting an adversarial domain adaptation approach using a standard domain discriminator. The third and last rows show the obtained results when using the proposed approach using a 1-Wasserstein distance and a Fréchet distance, respectively. It can be clearly seen that by leveraging the classifier as a discriminator, the performance of classification are generally improved in the presence of a domain shift. More specifically, an overall enhancement of 5.79%, 0.92%, and 2.89% can be seen in terms of mAP for AID \rightarrow UCM, UCM \rightarrow AID and UCM \rightarrow DFC, respectively, when compared to a classical adversarial approach incorporating an additional domain discriminator. However,

Table 1: Comparison with the state-of-the-art in terms of number of model parameters (in millions), and % scores for mAP, per-class averages (CP, CR, CF1) and per-example/overall averages (OP, OR, OF1) for UCM and AID datasets. Two settings are considered, *i.e.*, AID \rightarrow UCM and UCM \rightarrow AID. Best results are highlighted in **bold**.

Category	Method	# params	AID \rightarrow UCM							UCM \rightarrow AID						
			mAP	CP	CR	CF1	OP	OR	OF1	mAP	CP	CR	CF1	OP	OR	OF1
MLIC	DELTA [Yu <i>et al.</i> , 2019]	134.7	26.16	15.23	28.79	19.92	47.48	54.69	50.83	31.83	34.46	15.13	20.64	51.02	34.65	41.27
	KSSNET [Wang <i>et al.</i> , 2020]	44.9	20.89	12.32	24.89	16.48	50.79	55.31	50.79	26.45	7.12	9.22	8.03	58.84	24.87	34.97
	TRESNET-L [Ridnik <i>et al.</i> , 2021b]	53.8	37.03	29.6	34.04	31.33	48.45	69.59	57.13	33.98	15.97	17.66	16.77	54.80	36.09	43.52
	ASL [Ridnik <i>et al.</i> , 2021a]	53.8	12.33	16.15	30.46	21.11	38.26	79.25	51.61	39.79	53.27	31.06	39.24	78.79	44.99	57.28
DA	CDAN [Long <i>et al.</i> , 2018]	61.0	39.31	48.92	21.72	30.08	80.94	44.24	57.21	39.31	48.92	21.72	30.08	80.94	44.24	57.21
	MCD [Saito <i>et al.</i> , 2018]	44.6	40.57	47.39	16.61	26.36	73.37	31.7	45.59	38.00	30.67	18.11	22.77	80.69	35.31	49.12
	DA-MAIC [Lin <i>et al.</i> , 2021]	44.9	45.51	48.76	43.78	46.13	74.08	80.65	77.23	51.21	59.08	36.66	45.25	82.94	65.08	72.93
	Ours	DDA-MLIC	31.4	60.41	56.17	48.69	47.79	65.35	73.47	69.17	56.29	60.54	21.97	29.09	96.59	31.93

Table 2: Comparison with the state-of-the-art in terms of number of model parameters (in millions), and % scores for mAP, per-class averages (CP, CR, CF1) and per-example/overall averages (OP, OR, OF1) for UCM, DFC and AID. Two settings are considered, *i.e.*, UCM \rightarrow DFC and AID \rightarrow DFC. Best results are highlighted in **bold**.

Category	Method	# params	UCM \rightarrow DFC							AID \rightarrow DFC						
			mAP	CP	CR	CF1	OP	OR	OF1	mAP	CP	CR	CF1	OP	OR	OF1
MLIC	DELTA [Yu <i>et al.</i> , 2019]	134.7	44.135	19.66	20.16	19.91	38.9	13.36	19.83	51.59	37.75	51.57	43.6	33.8	37.96	35.76
	KSSNET [Wang <i>et al.</i> , 2020]	44.9	42.996	9.22	33.33	14.44	27.57	20.77	23.7	45.17	20.05	38.34	26.33	28.83	24.42	26.44
	TRESNET-L [Ridnik <i>et al.</i> , 2021b]	53.8	53.773	35.13	17.8	23.63	40.19	16.34	23.23	62.36	44.64	55.54	49.49	32.42	36.55	34.36
	ASL [Ridnik <i>et al.</i> , 2021a]	53.8	61.995	39.49	28.51	33.11	37.83	24.09	29.43	58.26	35.99	40.54	38.13	34.9	37.62	36.21
DA	CDAN [Long <i>et al.</i> , 2018]	61.0	55.386	25.29	27.84	26.5	35.71	24.48	29.05	57.53	36.65	51.87	44.94	31.67	33.91	32.75
	MCD [Saito <i>et al.</i> , 2018]	44.6	43.561	19.19	18.97	19.08	27.8	23.86	25.68	44.41	22.04	50.48	30.69	28.56	32.23	30.28
	DA-MAIC [Lin <i>et al.</i> , 2021]	44.9	68.663	42.28	33.55	37.41	43.85	25.44	23.86	72.99	46.18	59.62	52.05	46.12	42.73	44.36
	Ours	DDA-MLIC	31.4	71.89	72.56	49.2	45.85	61.13	52.35	56.4	59.93	50.1	42.98	38.29	55.35	48.09

Table 3: Comparison with the state-of-the-art in terms of mAP and number of model parameters for urban street datasets *i.e.*, GTA5 \rightarrow CityScapes. *Since the results for this setting is not provided in the original paper, we implement and retrain DA-MAIC [Lin *et al.*, 2021].

Method	# params	mAP
DA-MAIC* [Lin <i>et al.</i> , 2021]	44.9	52.32
DDA-MLIC (Ours)	31.4	64.07

Table 4: Ablation study (w/o: without, w/: with). The reported % scores are mAP.

Methods	AID \rightarrow UCM	UCM \rightarrow AID	UCM \rightarrow DFC	AID \rightarrow DFC
Ours. w/o DA [†]	58.34	51.87	66.77	53.67
Ours w/ Discr. [†]	54.62 (-3.72)	55.37 (+3.5)	69.0 (+2.23)	60.84 (+7.17)
Ours. w/ 1-Wasserstein [†]	58.37 (+3.75)	53.67 (-1.7)	71.45 (+2.45)	50.93 (-9.91)
Ours. w/ Fréchet dist.	60.41 (+2.04)	56.29 (+2.62)	71.89 (+0.44)	58.93 (+8.0)

[†]Reproduced results

a performance decrease of 1.91% can be observed for AID \rightarrow DFC. This is in line with the earlier observation in Table 2 and suggests that this might be due to the large class imbalance in the AID dataset.

Finally, the benefit of using a Fréchet distance [Dowson and Landau, 1982] instead of a 1-Wasserstein distance [Arjovsky *et al.*, 2017] is evaluated experimentally. Compared to the standard 1-Wasserstein distance, the Fréchet distance incorporates the second-order statistics, *i.e.*, the variance, for computing the distance between two Gaussian distributions. This distance choice significantly improves the performance by 2.04%, 2.62%, 0.44%, and 8.00% in terms of mAP for AID \rightarrow UCM, UCM \rightarrow AID, UCM \rightarrow DFC and UCM \rightarrow DFC, respectively.

6 Conclusion

In this paper, a discriminator-free UDA approach for MLIC has been proposed. In contrast to existing methods which

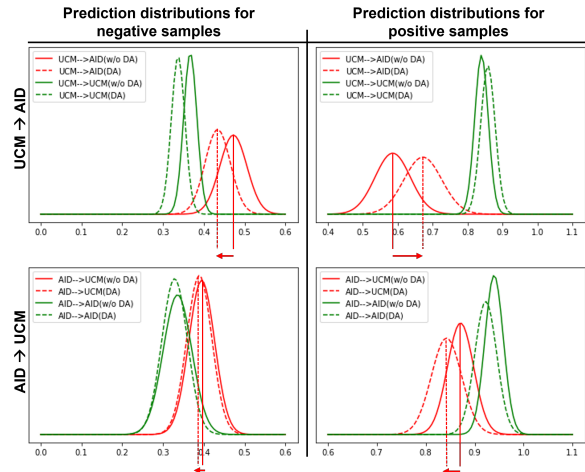


Figure 4: Qualitative analysis: Visualization of the prediction distributions before (solid line) and after (dotted line) domain adaptation for source (green) and target (red).

use an additional discriminator that is trained adversarially, our method leverages the task-specific classifier for implicitly discriminating between source and target domains. This strategy is proposed to avoid decoupling the classification and the discrimination tasks, while reducing the number of required network parameters. To achieve this, the adversarial loss has been redefined using a Fréchet distance between the corresponding GMM components estimated from the classifier probability predictions. We have demonstrated that the proposed approach achieves state-of-the-art results on three datasets, while considerably decreasing the size of the network. In future works, we will investigate a differentiable strategy for fitting the GMM for a fully end-to-end training of the network.

References

- [Arjovsky *et al.*, 2017] Martin Arjovsky, Soumith Chintala, and Léon Bottou. Wasserstein generative adversarial networks. In *ICML*, pages 214–223. PMLR, 2017.
- [Bell *et al.*, 2016] Sean Bell, C Lawrence Zitnick, Kavita Bala, and Ross Girshick. Inside-outside net: Detecting objects in context with skip pooling and recurrent neural networks. In *CVPR*, pages 2874–2883, 2016.
- [Chaudhuri *et al.*, 2017] Bindita Chaudhuri, Begüm Demir, Subhasis Chaudhuri, and Lorenzo Bruzzone. Multilabel remote sensing image retrieval using a semisupervised graph-theoretic method. *IEEE Transactions on Geoscience and Remote Sensing*, 56(2):1144–1158, 2017.
- [Chen *et al.*, 2022] Lin Chen, Huaian Chen, Zhixiang Wei, Xin Jin, Xiao Tan, Yi Jin, and Enhong Chen. Reusing the task-specific classifier as a discriminator: Discriminator-free adversarial domain adaptation. In *CVPR*, pages 7181–7190, 2022.
- [Cordts *et al.*, 2016] Marius Cordts, Mohamed Omran, Sebastian Ramos, Timo Rehfeld, Markus Enzweiler, Rodrigo Benenson, Uwe Franke, Stefan Roth, and Bernt Schiele. The cityscapes dataset for semantic urban scene understanding. In *CVPR*, pages 3213–3223, 2016.
- [Dowson and Landau, 1982] DC Dowson and BV Landau. The fréchet distance between multivariate normal distributions. *Journal of multivariate analysis*, 12(3):450–455, 1982.
- [Du *et al.*, 2021] Zhekai Du, Jingjing Li, Hongzu Su, Lei Zhu, and Ke Lu. Cross-domain gradient discrepancy minimization for unsupervised domain adaptation. In *Proceedings of the IEEE/CVF conference on computer vision and pattern recognition*, pages 3937–3946, 2021.
- [Everingham *et al.*, 2010] Mark Everingham, Luc Van Gool, Christopher KI Williams, John Winn, and Andrew Zisserman. The pascal visual object classes (voc) challenge. *International journal of computer vision*, 88(2):303–338, 2010.
- [Ganin *et al.*, 2016] Yaroslav Ganin, Evgeniya Ustinova, Hana Ajakan, Pascal Germain, Hugo Larochelle, François Laviolette, Mario Marchand, and Victor Lempitsky. Domain-adversarial training of neural networks. *JMLR*, 17(1):2096–2030, 2016.
- [He *et al.*, 2016] Kaiming He, Xiangyu Zhang, Shaoqing Ren, and Jian Sun. Deep residual learning for image recognition. In *CVPR*, pages 770–778, 2016.
- [Hua *et al.*, 2019] Yuansheng Hua, Lichao Mou, and Xiao Xiang Zhu. Recurrently exploring class-wise attention in a hybrid convolutional and bidirectional lstm network for multi-label aerial image classification. *ISPRS journal of photogrammetry and remote sensing*, 149:188–199, 2019.
- [Hua *et al.*, 2020] Yuansheng Hua, Lichao Mou, and Xiao Xiang Zhu. Relation network for multilabel aerial image classification. *IEEE Transactions on Geoscience and Remote Sensing*, 58(7):4558–4572, 2020.
- [Kang *et al.*, 2019] Guoliang Kang, Lu Jiang, Yi Yang, and Alexander G Hauptmann. Contrastive adaptation network for unsupervised domain adaptation. In *Proceedings of the IEEE/CVF Conference on Computer Vision and Pattern Recognition*, pages 4893–4902, 2019.
- [Lee *et al.*, 2019] Chen-Yu Lee, Tanmay Batra, Mohammad Haris Baig, and Daniel Ulbricht. Sliced wasserstein discrepancy for unsupervised domain adaptation. In *CVPR*, pages 10285–10295, 2019.
- [Li *et al.*, 2016] Yining Li, Chen Huang, Chen Change Loy, and Xiaoou Tang. Human attribute recognition by deep hierarchical contexts. In *ECCV*, pages 684–700. Springer, 2016.
- [Li *et al.*, 2019] Yunsheng Li, Lu Yuan, and Nuno Vasconcelos. Bidirectional learning for domain adaptation of semantic segmentation. In *Proceedings of the IEEE/CVF Conference on Computer Vision and Pattern Recognition*, pages 6936–6945, 2019.
- [Lin *et al.*, 2014] Tsung-Yi Lin, Michael Maire, Serge Belongie, James Hays, Pietro Perona, Deva Ramanan, Piotr Dollár, and C Lawrence Zitnick. Microsoft coco: Common objects in context. In *ECCV*, pages 740–755. Springer, 2014.
- [Lin *et al.*, 2021] Dan Lin, Jianzhe Lin, Liang Zhao, Z Jane Wang, and Zhikui Chen. Multilabel aerial image classification with unsupervised domain adaptation. *IEEE Transactions on Geoscience and Remote Sensing*, 60:1–13, 2021.
- [Long *et al.*, 2015] Mingsheng Long, Yue Cao, Jianmin Wang, and Michael Jordan. Learning transferable features with deep adaptation networks. In *International conference on machine learning*, pages 97–105. PMLR, 2015.
- [Long *et al.*, 2018] Mingsheng Long, Zhangjie Cao, Jianmin Wang, and Michael I Jordan. Conditional adversarial domain adaptation. *NeurIPS*, 31, 2018.
- [Murez *et al.*, 2018] Zak Murez, Soheil Kolouri, David Kriegman, Ravi Ramamoorthi, and Kyungnam Kim. Image to image translation for domain adaptation. In *Proceedings of the IEEE Conference on Computer Vision and Pattern Recognition*, pages 4500–4509, 2018.
- [Pei *et al.*, 2018] Zhongyi Pei, Zhangjie Cao, Mingsheng Long, and Jianmin Wang. Multi-adversarial domain adaptation. In *AAAI*, 2018.
- [Pham *et al.*, 2021] Duc Duy Pham, SM Koesnadi, Gurbandurdy Dovletov, and Josef Pauli. Unsupervised adversarial domain adaptation for multi-label classification of chest x-ray. In *ISBI*, pages 1236–1240. IEEE, 2021.
- [Reynolds, 2009] Douglas A Reynolds. Gaussian mixture models. *Encyclopedia of biometrics*, 741(659-663), 2009.
- [Richter *et al.*, 2016] Stephan R Richter, Vibhav Vineet, Stefan Roth, and Vladlen Koltun. Playing for data: Ground truth from computer games. In *ECCV*, pages 102–118. Springer, 2016.
- [Ridnik *et al.*, 2021a] Tal Ridnik, Emanuel Ben-Baruch, Nadav Zamir, Asaf Noy, Itamar Friedman, Matan Protter, and

- Lihi Zelnik-Manor. Asymmetric loss for multi-label classification. In *ICCV*, pages 82–91, 2021.
- [Ridnik *et al.*, 2021b] Tal Ridnik, Hussam Lawen, Asaf Noy, Emanuel Ben Baruch, Gilad Sharir, and Itamar Friedman. Tresnet: High performance gpu-dedicated architecture. In *WACV*, pages 1400–1409, 2021.
- [Saito *et al.*, 2018] Kuniaki Saito, Kohei Watanabe, Yoshitaka Ushiku, and Tatsuya Harada. Maximum classifier discrepancy for unsupervised domain adaptation. In *CVPR*, pages 3723–3732, 2018.
- [Shao *et al.*, 2015] Jing Shao, Kai Kang, Chen Change Loy, and Xiaogang Wang. Deeply learned attributes for crowded scene understanding. In *CVPR*, pages 4657–4666, 2015.
- [Singh *et al.*, 2023] Indel Pal Singh, Enjie Ghorbel, Oyebede Oyedotun, and Djamila Aouada. Multi-label image classification using adaptive graph convolutional networks: from a single domain to multiple domains. *arXiv preprint arXiv:2301.04494*, 2023.
- [Sun *et al.*, 2019] Yu Sun, Eric Tzeng, Trevor Darrell, and Alexei A Efros. Unsupervised domain adaptation through self-supervision. *arXiv preprint arXiv:1909.11825*, 2019.
- [Tang and Jia, 2020] Hui Tang and Kui Jia. Discriminative adversarial domain adaptation. In *Proceedings of the AAAI Conference on Artificial Intelligence*, volume 34, pages 5940–5947, 2020.
- [Tzeng *et al.*, 2014] Eric Tzeng, Judy Hoffman, Ning Zhang, Kate Saenko, and Trevor Darrell. Deep domain confusion: Maximizing for domain invariance. *CoRR*, abs/1412.3474, 2014.
- [Wang *et al.*, 2020] Ya Wang, Dongliang He, Fu Li, Xiang Long, Zhichao Zhou, Jinwen Ma, and Shilei Wen. Multi-label classification with label graph superimposing. In *AAAI*, pages 12265–12272, 2020.
- [Xia *et al.*, 2017] Gui-Song Xia, Jingwen Hu, Fan Hu, Baoguang Shi, Xiang Bai, Yanfei Zhong, Liangpei Zhang, and Xiaoqiang Lu. Aid: A benchmark data set for performance evaluation of aerial scene classification. *IEEE Transactions on Geoscience and Remote Sensing*, 55(7):3965–3981, 2017.
- [Yang and Newsam, 2010] Yi Yang and Shawn Newsam. Bag-of-visual-words and spatial extensions for land-use classification. In *Proceedings of the 18th SIGSPATIAL international conference on advances in geographic information systems*, pages 270–279, 2010.
- [Yu *et al.*, 2019] Wan-Jin Yu, Zhen-Duo Chen, Xin Luo, Wu Liu, and Xin-Shun Xu. Delta: A deep dual-stream network for multi-label image classification. *Pattern Recognition*, 91:322–331, 2019.
- [Zhang *et al.*, 2019] Yuchen Zhang, Tianle Liu, Mingsheng Long, and Michael Jordan. Bridging theory and algorithm for domain adaptation. In *International Conference on Machine Learning*, pages 7404–7413. PMLR, 2019.